Electronic Supplementary Material (ESI) for ChemComm.

Local tensile strain boosts the electrocatalytic ammonia oxidation reaction

Yongzhen Jin[a,c,d], Yang Liu[a,c,d], Ruyan Wu[c,d,e], Jianhui Wang*[a,b,c,d]

[a.] School of Materials Science and Engineering, Zhejiang University, Hangzhou 310027, China

[b.] Research Center for Industries of the Future, Westlake University, Hangzhou 310030, China

[c.] Key Laboratory of 3D Micro/Nano Fabrication and Characterization of Zhejiang Province, School of Engineering, Westlake University, Hangzhou 310030, China

[d.] Institute of Advanced Technology, Westlake Institute for Advanced Study, Hangzhou 310024, China

[e.] School of Automotive Engineering, Hangzhou Polytechnic, Hangzhou 311402, China

Corresponding Author

Email: wangjianhui@westlake.edu.cn

1. Experimental Section

1.1 Materials

Nickel foam (NF, Canrd); $NaH_2PO_2 \cdot H_2O$ (Aladdin, 99.0%); $Ni(NO_3)_2 \cdot 6H_2O$ (Aladdin, > 99.9%); $Ni(OH)_2$ (Adamas, 99%); $CO(NH_2)_2$ (Aladdin, > 99.5%); NH_4F (Aladdin, 98.0 %); HCl (Guangfu, 37%); NaOH (MACKLIN, ≥ 99.8 %); $NH_4 \cdot Cl$ (MACKLIN, ≥ 99.5%); $^{15}NH_4 \cdot Cl$ (Aladdin, ≥ 98.0 %).

1.2 Sample preparation

(1) Preparation of nickel hydroxide precursor on the nickel foam

Firstly, a piece of nickel foam (3 cm × 4 cm) was treated in 3 M HCl solution by ultrasonication for 15 minutes, then washing with deionized water several times until the PH = 7. Finally, it was dried in an oven at 60 ℃ for 6 hours.

In a typical procedure, $Ni(NO_3)_2 \cdot 6H_2O$ (5 mmol), NH_4F (8 mmol) and $Co(NH_2)_2$ (20 mmol) were dissolved in 40 mL deionized water. The resulting solution was transferred to a 50 mL Teflon-lined stainless-steel autoclave. Then a piece of treated nickel foam was immersed into the solution. The autoclave was sealed and heated at 120 ℃ for 10 hours in an oven. After the autoclave cooled down to room temperature, the hydroxide precursor was taken out and washed with deionized water for several times and dried at 60 ℃ for 6 hours.

(2) Preparation of Ni_2P on the nickel foam

Ni_2P was prepared by mixing a piece of nickel foam (2 cm × 4 cm, without any treatment) with $NaH_2PO_2 \cdot H_2O$ (1.0 g) in an alumina boat. Then the alumina boat was sealed with aluminum foil and subjected to annealing in Ar atmosphere at 300 °C for one hour with a heating speed of 2 ℃ min^{-1}. After cooling down to room temperature, the product was taken out and rinsed with deionized water and dried at 60 ℃ for 6 hours.

(3) Preparation of P vacancies containing Ni_2P (V-Ni_2P) on the nickel foam

The hydroxide precursor was placed in an alumina boat. Another alumina boat containing 1.0 g $NaH_2PO_2 \cdot H_2O$ was placed at the upstream of the tube furnace. Then the two alumina boats were calcined at 300 ℃ for 2 hours with a heating speed of 2 ℃ min^{-1} in Ar atmosphere with a gas flow rate of 20 mL min^{-1} and cooled down to room temperature naturally.

(4) Preparation of tst-$Ni(OH)_2$ on Nickel Foam

Tst-$Ni(OH)_2$ was prepared by carried out 20 cycles CV scans using V-Ni_2P as working electrode, Hg/HgO as reference electrode and graphite rod as counter electrode in the electrolyte of 1.5 M NaOH + 0.5 M NH_3 with a scan rate of 25 mV s^{-1}.

(5) Preparation of ust-$Ni(OH)_2$ on Nickel Foam

Ust-$Ni(OH)_2$ was prepared by carried out 20 cycles CV scans using Ni_2P as working electrode, Hg/HgO as reference electrode and graphite rod as counter electrode in the electrolyte of 1.5 M NaOH + 0.5 M NH_3 with a scan rate of 25 mV s^{-1}.

1.3 Material characterizations

X-ray powder diffraction (XRD) patterns were obtained on a Bruker D8 Advance powder diffractometer, using Cu Kα (λ = 1.5418 Å) as the radiation source. Raman spectra were examined by a Raman spectrometer (Alpha300RAS) with an exciting laser of 532 nm. The scanning electron microscopy (SEM) images were taken on a Hitachi Regulus 8230. The images of transmission electron microscopy (TEM) and high-resolution transmission electron microscopy (HRTEM) as well as the elemental mapping were obtained by using a Talos F200X G2 electron microscope (Thermo Fisher Scientific) operated at 200 kV. The electron paramagnetic resonance (EPR) spectra were recorded on a Bruker A300 spectrometer. X-ray photoelectron spectroscopy (XPS) measurements were performed on a Thermo Fisher ESCALAB Xi+. The binding energies were calibrated using C 1s peak at 284.8 eV as standard. Ion chromatography (Thermo Fisher ICS 6000) was applied to identify the liquid products in the electrolyte.

1.4 Electrochemical measurements

Electrochemical measurements were conducted in a three-electrode cell on a workstation (CHI660E, Shanghai, China) using a graphite rod as the counter electrode, a Hg/HgO as the reference electrode and the as-prepared Ni-based catalysts as the working electrode. Before the measurement, the electrolyte (1.5 M NaOH or 1.5 M NaOH + 0.5 M NH_4Cl) was bubbled with an Argon gas flow for 20 min to remove air. CV tests were performed at a scan rate of 25 mV s^{-1}. The electrochemically active surface areas (ECSA) of the electrocatalysts were evaluated by the equation of $ECSA = C_{dl} / C_s$. C_s is 40 μF cm^{-2} as a typical value of the specific capacitance of metallic surfaces in 1 M NaOH. The C_{dl} was half of the liner slope, which was obtained by plotting the $\Delta j = ja - jc$ at -0.73 V vs. Hg/HgO against the scan rate (10, 30, 50, 70, 90 mV s^{-1}, respectively). All the electrochemical measurements were tested in a single cell unless specified otherwise.

1.5 In situ Raman analysis

In situ Raman measurements were performed in a homemade three-electrode cell (MicroElab, R-Cata-S). The tst-$Ni(OH)_2$ or ust-$Ni(OH)_2$ on Ni foam, Hg/HgO electrode and Pt wire were used as the working electrode, the reference electrode, and the counter electrode, respectively. The Raman spectra was tested on a Raman spectrometer (Alpha300R) with an exciting laser of 532 nm during CA test at different potentials.

1.6 In situ DEMS analysis

Differential electrochemical mass spectrometry (DEMS, Linglu Shanghai) measurements were carried out for in situ analysis of gas products during EAOR, such as N_2 (28 m/z), $^{15}N_2$ (30 m/z), $^{15}N_2N_4$ (34 m/z). The working electrode was tst-$Ni(OH)_2$ or ust-$Ni(OH)_2$ on Ni foam. The PTFE membrane (50 μm thickness, 20 nm pore) that only allows the penetration of volatile and hydrophobic species was used in the measurements. In situ DEMS is used to detect volatile products and intermediates in the electrolyte (directly generated on the surface of the catalyst).

1.7 On line MS

Various gas products were analyzed using a Hiden Analytical Mass Spectrometer (QIC-20), which equipped with capillary, quadrupole mass analyser and Faraday/secondary electron multiplier detectors. During EAOR test, pure Ar was used as the carrier gas with a flow rate of 25 mL min^{-1}. MID mode was applied to monitor various possible gases, such as H_2 (m/z: 2), N_2 (m/z: 28), O_2 (m/z: 32), NO (m/z: 30), NO_2 (m/z: 46) and N_2O (m/z: 44). On line MS is used to detect the gas products that have separated form the electrolyte.

1.8 Collection of gas products by drainage method

A sealed H-shaped electrochemical cell was used for collection of gas products during a one-hour test at 0.6 V vs. Hg/HgO, where the tst-$Ni(OH)_2$ or ust-$Ni(OH)_2$ on Ni foam, Hg/HgO electrode, and the graphite rod were used as the working electrode, the reference electrode, and the counter electrode, respectively.

1.9 Calculation of the faradaic efficiency

The faradaic efficiency of H_2 was calculated according to the equation (1):

$$H_2 \text{ faradaic efficiency} = \frac{2 \times V_{H_2} \times F}{V_m \times Q} \times 100\% \quad (1)$$

Where V_{H_2} is the volume of H_2 collected by the drainage method; V_m is the molar volume of the gas (22.4 L mol^{-1}); F is the faraday constant (96485 C mol^{-1}), Q is the total charge consumed in the measurement.

The faradaic efficiency of N_2 was calculated according to the equation (2):

$$N_2 \text{ faradaic efficiency} = \frac{6 \times V_{N_2} \times F}{V_m \times Q} \times 100\% \quad (2)$$

Where V_{N_2} is the volume of N_2 collected by the drainage method; V_m is the molar volume of the gas (22.4 L mol^{-1}); F is the faraday constant (96485 C mol^{-1}), Q is the total charge consumed in the measurement.

The faradaic efficiencies of NO_2^- and NO_3^- were calculated according to the equation (3) and (4), respectively:

$$NO2- \ faradaic\ efficiency = \frac{6 \times C_{NO2-} \times V \times F}{M \times Q} \times 100\% \quad (3)$$

$$NO3- \ faradaic\ efficiency = \frac{8 \times C_{NO3-} \times V \times F}{M \times Q} \times 100\% \quad (4)$$

Where C_{NO2-} and C_{NO3-} are the concentration of NO_2^- and NO_3^- ion produced in the electrolyte determined by ion chromatography, respectively; V is the volume of electrolyte (30 mL); M is the molar mass of $NO_2^-$and NO_3^-; F is the faradaic constant (96485 C mol^{-1}), Q is the total charge consumed in the measurement.

2. Supplementary Figures.

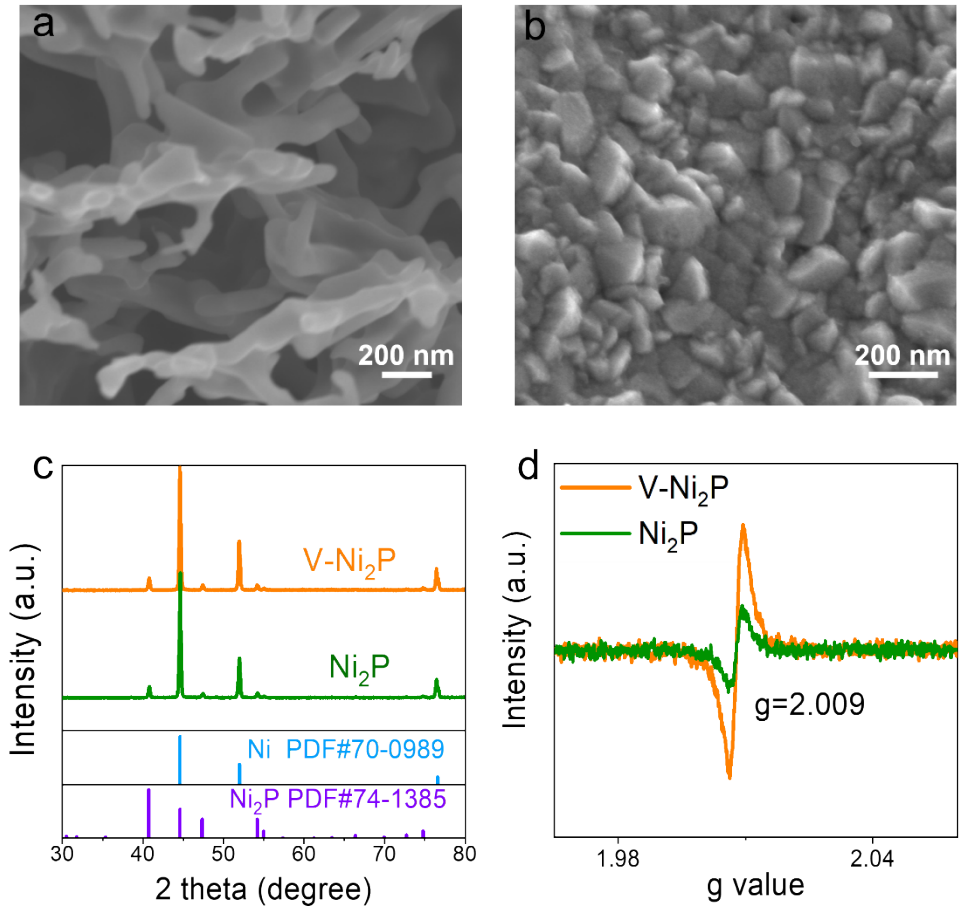

Figure S1. (a) SEM image of V-Ni_2P. (b) SEM image of Ni_2P. (c) XRD patterns of V-Ni_2P and Ni_2P. (d) EPR spectra of V-Ni_2P and Ni_2P. The EPR spectra show a considerably higher signal at g=2.009 for the V-Ni_2P sample than that for the Ni_2P sample, evidencing that the former contains a significant concentration of P vacancies while few P vacancies in the latter.

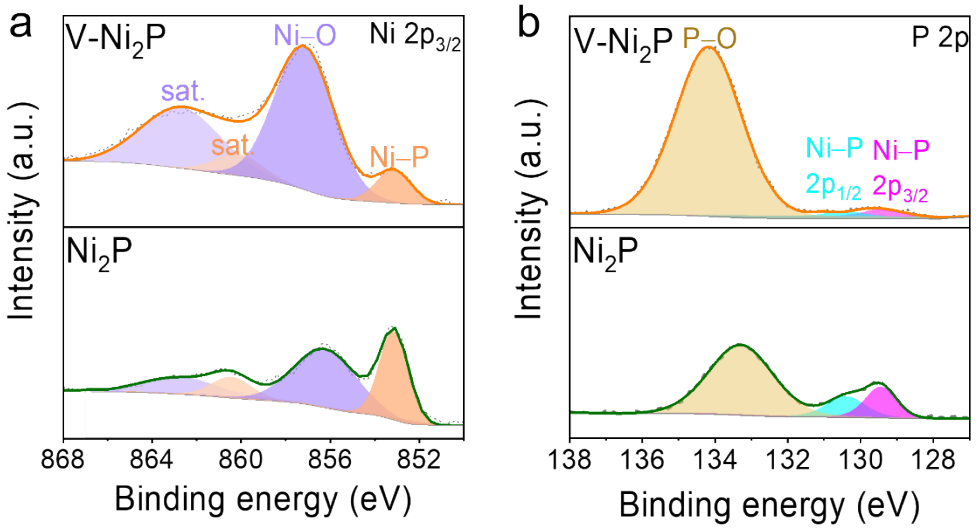

Figure S2. (a) Ni $2p_{3/2}$ and (b) P 2p XPS spectra of V-Ni_2P and Ni_2P before surface reconstruction.

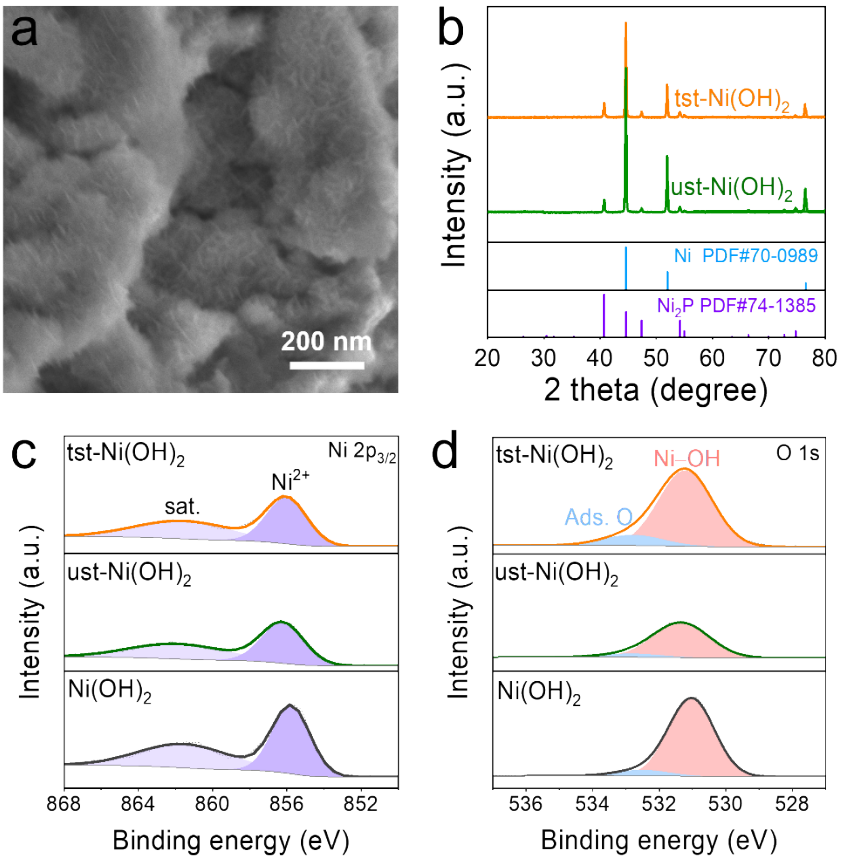

Figure S3. (a) SEM image of ust-$Ni(OH)_2$. (b) XRD patterns of as-prepared tst-$Ni(OH)_2$ and ust-$Ni(OH)_2$. These XRD patterns show almost identical with those of the V-Ni_2P and P-Ni_2P samples, indicating the reconstructed $Ni(OH)_2$ nanosheets are amorphous. (c) Ni $2p_{3/2}$ XPS spectra of tst-$Ni(OH)_2$, ust-$Ni(OH)_2$ and pristine $Ni(OH)_2$. (d) O1s XPS spectra of tst-$Ni(OH)_2$, ust-$Ni(OH)_2$ and pristine $Ni(OH)_2$.

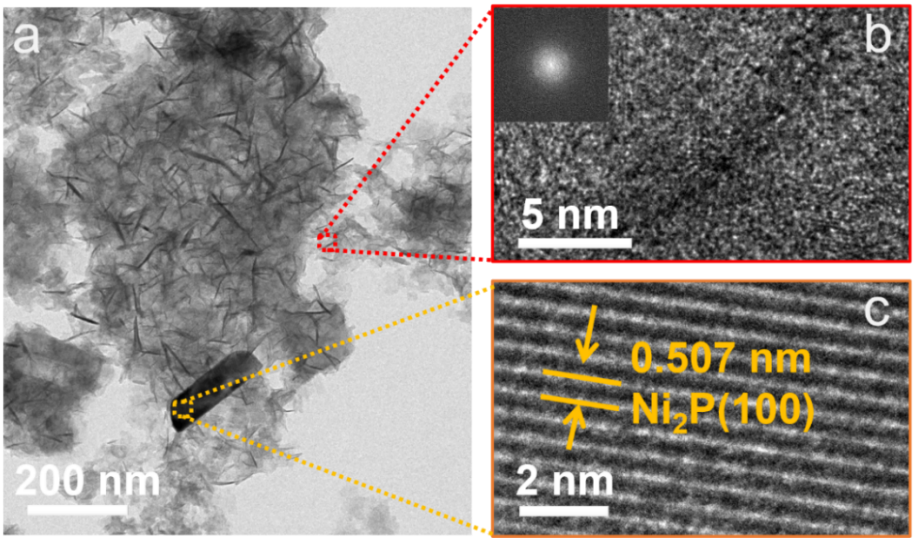

Figure S4. (a) TEM image of the tst-$Ni(OH)_2$ sample after sonicating in ethanol. (b) HRTEM image of the amorphous nanosheets covered on the tst-$Ni(OH)_2$ sample. Inset displays the derived FFT pattern. (c) HRTEM image of the crystalline Ni_2P nanorods core in the tst-$Ni(OH)_2$ sample.

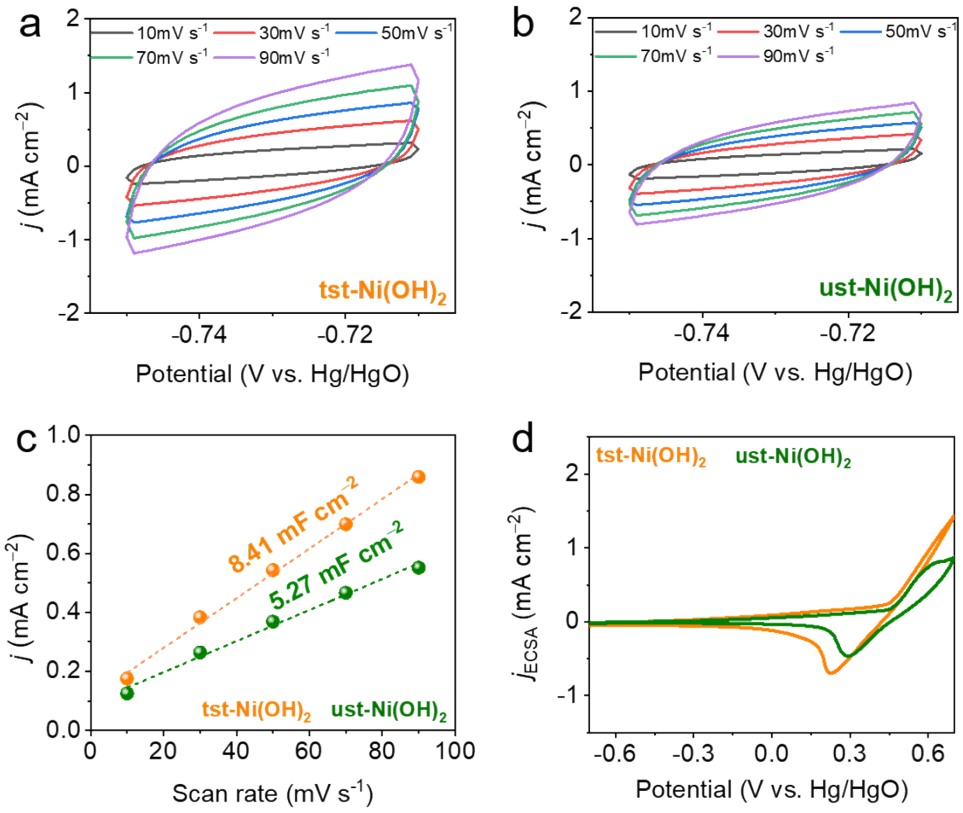

Figure S5. (a) CV curves of tst-$Ni(OH)_2$ at -0.75 ~ -0.70 V vs. Hg/HgO at different scanning rates. (b) CV curves of ust-$Ni(OH)_2$ at -0.75 ~ -0.70 V vs. Hg/HgO at different scanning rates. (c) Plots of the current density versus the scanning rate to determine the double layer capacitance (C_{dl}) of tst-$Ni(OH)_2$ and ust-$Ni(OH)_2$. (d) ECSA-normalized CV curves of tst-$Ni(OH)_2$ and ust-$Ni(OH)_2$. The electrolyte is an aqueous solution of 1.5 M NaOH + 0.5 M NH_3.

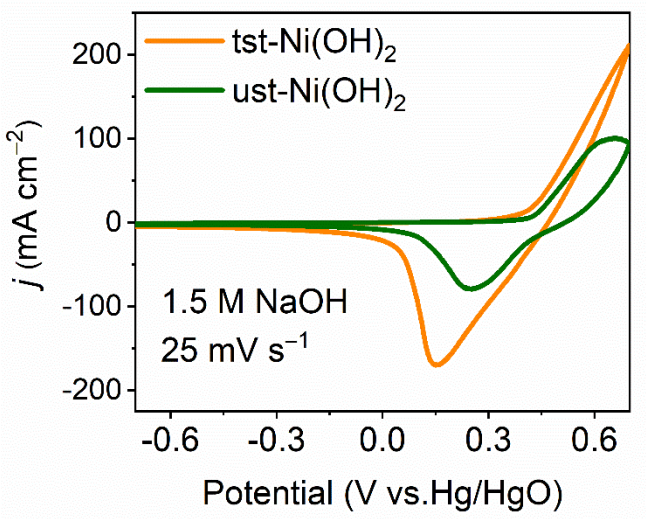

Figure S6. CV curves of the tst-$Ni(OH)_2$ and ust-$Ni(OH)_2$ in the electrolyte of 1.5 M NaOH.

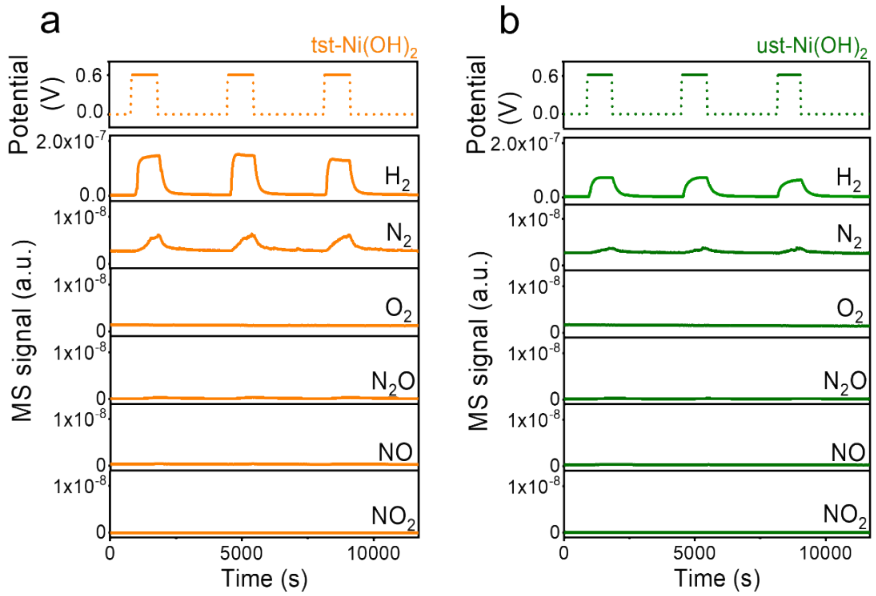

Figure S7. (a and b) Online MS signals of gas product for tst-Ni(OH)$_2$ (a) and ust-Ni(OH)$_2$ (b) in the electrolyte of 1.5 M NaOH + 0.5 M NH$_3$ at 0.6 V vs. Hg/HgO.

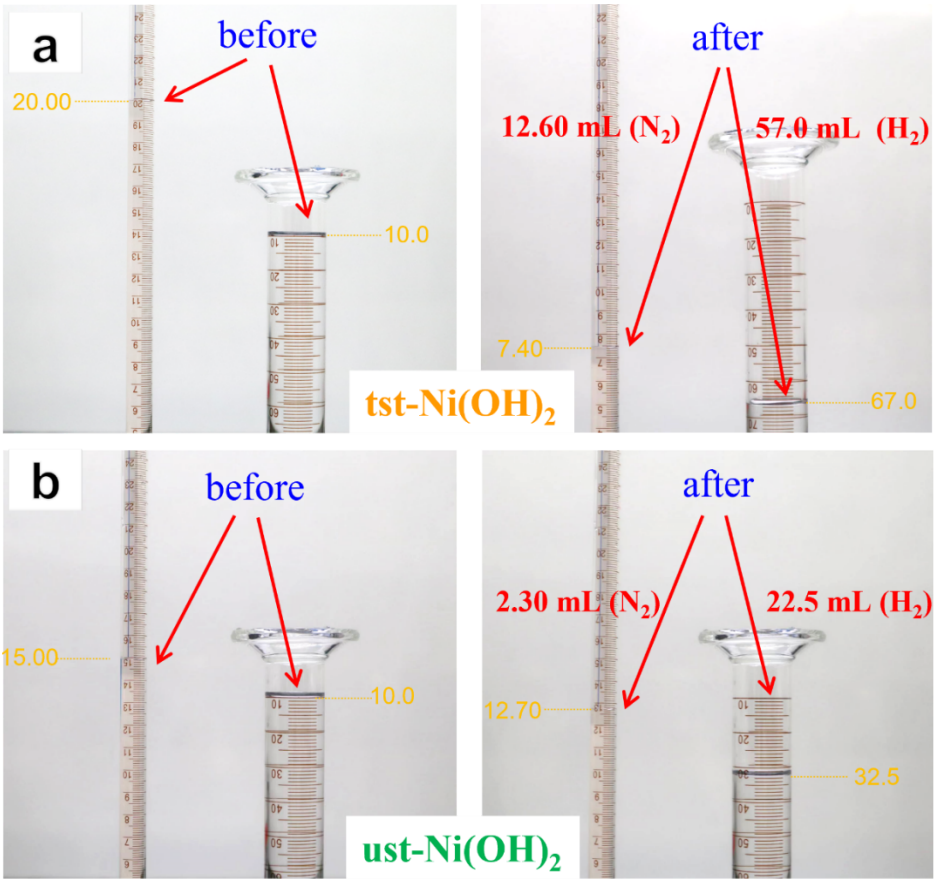

Figure S8. Collection of the cathodic (H$_2$) and anodic (N$_2$) gas products for tst-Ni(OH)$_2$ (a) and ust-Ni(OH)$_2$ (b) catalyzed EAOR by the drainage method. The gas products were generated during a one-hour test at 0.6 V vs. Hg/HgO.

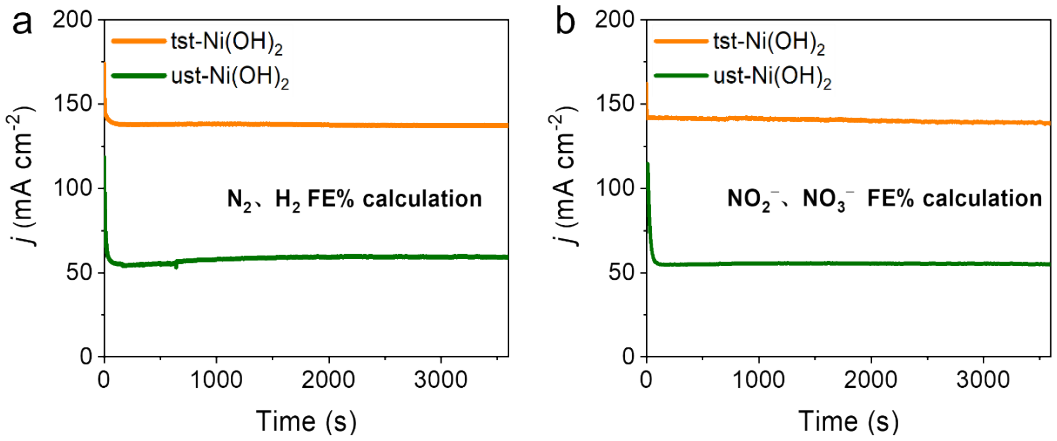

Figure S9. (a) CA tests for the faradaic efficiency calculations of N_2 and H_2. (b) CA tests for the faradaic efficiency calculations of NO_2^- and NO_3^-.

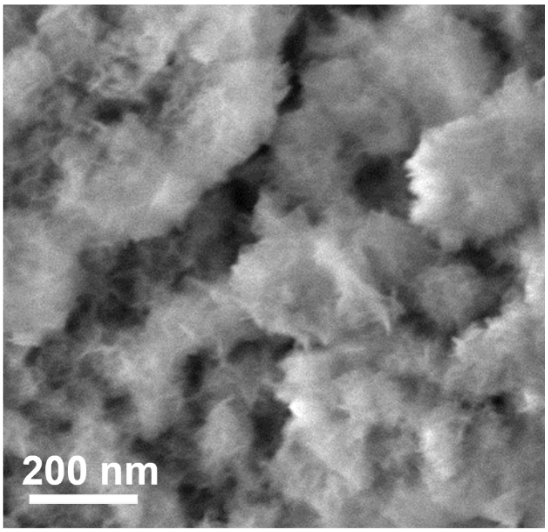

Figure S10. SEM image of tst-$Ni(OH)_2$ after 1000 hours' durability test.

3. Supplementary Tables.

Table S1. The concentration of PO_4^- in the electrolyte after surface reconstruction of V-Ni_2P.

Sample	c (PO_4^-) (mg L^{-1})
V-Ni_2P	95.81

Table S2. Electrochemical active surface area of various samples.

Sample	**tst-$Ni(OH)_2$**	**ust-$Ni(OH)_2$**
C_{dl} (mF cm^{-2})	8.41	5.27
ECSA (cm^2)	210.25	131.75

Table S3. Faradaic efficiencies of N_2 and H_2 in the tst-$Ni(OH)_2$ and ust-$Ni(OH)_2$ catalyzed EAOR.

Sample	Total charge (C)	V (N_2) (mL)	V (H_2) (mL)	Faradaic efficiency (N_2) (%)	Faradaic efficiency (H_2) (%)
tst-$Ni(OH)_2$	493.0	12.60 ± 0.05	57.0 ± 0.5	66.00 ± 0.26	99.5 ± 0.9
ust-$Ni(OH)_2$	195.0	2.30 ± 0.05	22.5 ± 0.5	30.50 ± 0.66	99.3 ± 2.2

The gas products of H_2 and N_2 were collected at 0.6 V vs. Hg/HgO for one hour.

Table S4. Faradaic efficiencies of $NO_2^-$and NO_3^- in the the tst-$Ni(OH)_2$ and ust-$Ni(OH)_2$ catalyzed EAOR.

Sample	Total charge (C)	c (NO_2^-) (mg L^{-1})	c (NO_3^-) (mg L^{-1})	Faradaic efficiency (NO_2^-) (%)	Faradaic efficiency (NO_3^-) (%)
tst-$Ni(OH)_2$	507.2	0.00	260.68	0.0	19.9
ust-$Ni(OH)_2$	201.0	5.83	287.12	2.0	55.4

The liquid products of NO_2^- and NO_3^- were collected at 0.6 V vs. Hg/HgO for one hour.